HHS Public Access

Author manuscript

J Neurochem. Author manuscript; available in PMC 2016 April 01.

Published in final edited form as:

J Neurochem. 2015 April ; 133(2): 167–173. doi:10.1111/jnc.13025.

Dopamine transporter oligomerization: Impact of combining protomers with differential cocaine analog binding affinities

Juan Zhen[*], **Tamara Antonio**[*], **Shu-Yuan Cheng**[+], **Solav Ali**[#], **Kymry T. Jones**[*], and **Maarten E. A. Reith**[*,$]

[*]Department of Psychiatry, New York University School of Medicine, New York, USA

[+]Department of Sciences, John Jay College of Criminal Justice, CUNY, NY, USA

[#]Department of Neuroscience and Physiology, New York University School of Medicine, New York, USA

[$]Department of Biochemistry and Molecular Pharmacology, New York University School of Medicine, New York, USA

Abstract

Previous studies point to quaternary assembly of dopamine transporters (DATs) in oligomers. However, it is not clear whether the protomers function independently in the oligomer. Is each protomer an entirely separate unit that takes up dopamine and is inhibited by drugs known to block DAT function? In this work, human embryonic kidney 293 cells were co-transfected with DAT constructs possessing differential binding affinities for the phenyltropane cocaine analog, [^{3}H]WIN35,428. It was assessed whether the binding properties in co-expressing cells capable of forming hetero-oligomers differ from those in preparations obtained from mixed singly transfected cells where such oligomers cannot occur. A method is described that replaces laborious "mixing" experiments with an in silico method predicting binding parameters from those observed for the singly expressed constructs. Among 5 pairs of constructs tested, statistically significant interactions were found between protomers of wild-type (WT) and D313N, WT and D345N, and WT and D436N. Compared with predicted K_d values of [^{3}H]WIN35,428 binding to the non-interacting pairs, the observed affinity of the former pair was increased 1.7 fold while the latter two were reduced 2.2 and 4.1 fold, respectively. This is the first report of an influence of protomer composition on the properties of a DAT inhibitor, indicating cooperativity within the oligomer.

Keywords

dopamine transporter oligomers; transporter point mutants; cocaine analog binding; CFT; WIN 35,428

Address correspondence to: Maarten E.A. Reith, Ph.D., Department of Psychiatry, Alexandria Center of Life Sciences, New York University, 450 E 29th Street, Room 803, New York, NY 10016. Tel.: 212 - 263 8267; Fax: 212 – 263 8183; Maarten.Reith@nyumc.org.

The authors have no conflicts of interest to declare.

Introduction

Abundant evidence points to the quaternary assembly of biogenic amine transporters into oligomers as studied with radiation inactivation, co-immunoprecipitation, Ni^{2+}-chromatography, cross-linking, and FRET (Berger *et al.* 1994; Milner *et al.* 1994; Hastrup *et al.* 2001; 2003; Sitte and Freissmuth 2003; Sorkina *et al.* 2003; Sitte *et al.* 2004; Just *et al.* 2004; Chen and Reith 2008; Li *et al.* 2010). Additional support for oligomerization in this family of proteins has come from dominant-negative mutants. Indeed, Kitayama et al. (1999) showed that a splice variant at the 3′-region of the norepinephrine transporter was functionally inactive and interfered with the wild-type (WT)-like transport activity of another splice variant. Similarly, Torres et al. (2003) reported a dominant-negative effect on WT dopamine transporter (DAT) activity by co-expression of WT with the inactive mutant Y335A or D79G. For Y335A, there is the caveat of possible channel-like properties, as discussed by Sitte et al. (2004), in which mutation-induced effects could impair electrochemical gradients and thereby the function of WT DAT. The present work reduces possible effects of mutant DAT constructs from electrochemical gradient changes by studying binding of the phenyltropane cocaine analog CFT ((−)-2-β-carbomethoxy-3-β-(4-fluorophenyl)tropane = WIN 35,428) (Li *et al.* 2010; Schmitt and Reith 2011) which is independent of membrane potential (Billaud *et al.* 1993; Chen and Reith 2004; Zhen *et al.* 2005). This measure is used here to assess whether protomers in an oligomeric DAT assembly can affect each other's function. To that end, we co-transfected human embryonic kidney (HEK) 293 cells with DAT constructs possessing differential binding affinity for [^{3}H]CFT. The main objective was to determine whether the formation of DAT hetero-oligomers in co-transfected cells results in inhibitor binding properties that differ from singly transfected cells. The present results document instances of protomer interactions altering the resultant CFT binding properties.

Materials and methods

Expression of DAT cDNA constructs, cell culture and transfection

Human embryonic kidney cells (HEK-293, ATCC CRL1573) were maintained in Dulbecc's modified Eagle's medium supplemented with 10% fetal calf serum at 37°C and 5% CO_2. For transient expression, total 16 μg of plasmid(s) and 40 μL of Lipofectamine 2000 (Invitrogen, Grand Island, NY) were used for transfection per 10-cm culture Petri dish of cells. To study whether protomers interacted, we co-transfected cells with two full-length DAT cDNA constructs, at 1:1 ratio (8 μg each) or with each construct (16 μg). Binding assays were performed approximately 48 hours after transfection. For "mixing" experiments (see below), stably expressing cell lines were used and prepared as described previously (Chen *et al.* 2001; Chen *et al.* 2004a; Chen *et al.* 2004b; Liang *et al.* 2009; Li *et al.* 2010).

Binding assays and data analysis

Saturation analysis of [^{3}H]WIN35,428 (CFT) binding to intact cells was measured in 96-well plates with modified Krebs–Ringer–HEPES buffer in triplicate as described in our previous work (Liang *et al.* 2009; Schmitt and Reith 2011). Increasing concentrations of non-radioactive CFT were included in the assay mixture to generate final CFT

concentrations of 2, 6, 14, 30, or 100 nM. Nonspecific binding was defined with 1 μM CFT. The equilibrium dissociation constant (K_d) for CFT binding, and the maximal CFT-binding capacity (B_{max}) were estimated by nonlinear regression fitting of data with RADLIG software (KELL program; Biosoft, Cambridge, UK). To detect the interaction between the promoters, K_d and B_{max} for [^{3}H]CFT binding were determined with whole cell suspensions prepared from hDAT stably-transfected (table 1) or transient-transfected HEK-293 cells (table 2) as indicated in text.

In the notation used by Rosenthal (Rosenthal 1967), [b_1] and [b_2] denote the concentration of ligand bound to population 1 and 2 of binding sites, i.e. [^{3}H]WIN35,428 bound to the two hDAT constructs. Thus, $[b_1]+[b_2]=[u]\times\left(\frac{B_{max1}}{K_{d1}+[u]}\right)+[u]\times\left(\frac{B_{max2}}{K_{d2}+[u]}\right)$ in which [u] is the concentration of free ligand (free [^{3}H]WIN35,428). For a graphical representation in a Scatchard plot, one can calculate for each concentration of CFT the x and y value of each data point as ([b_1] + [b_2]) and $\left(\frac{b_1}{[u]}+\frac{b_2}{[u]}\right)$ (Rosenthal 1967). The predicted specific values of [^{3}H] WIN 35,428 binding to non-interacting protomers were computed for each combination of WT and mutant DAT (simple mixing or co-transfection) from the observed K_d and B_{max} of each construct from the same set of one-site binding experiments. Since the total amount of DNA in co-transfection was kept the same as in single-transfection, half of each hDAT construct was used under the co-transfection conditions. Thus, in these cases, observed B_{max1} and B_{max2} values were divided by 2 in the above equations. The *in silico* generated data points (for 2, 6, 14, 30, or 100 nM CFT) were then subjected to LIGAND non-linear computer fitting (Kurian *et al.* 2009) to simulate a binding experiment on co-expressed DAT constructs forming hetero-oligomers consisting of non-interacting protomers. The results of this simulated experiment were then compared with observations on co-expressed DAT constructs or cell mixtures of cultures expressing each construct individually. Observed binding parameters were statistically compared with the corresponding predicted values by one-sample Student's t-test (two-sided); the null hypothesis (i.e., the observed binding parameter is equal to the predicted value) was rejected when $P < 0.05$. For graphical presentation, Scatchard plots were generated for constructs expressed separately and together, and for "mixing" experiments.

Surface DAT studied by biotinylation

In separate experiments, the effect of co-expressing one construct with another on surface DAT was assessed by biotinylation with SulfoLink NHS-SS-biotin (ThermoScientific, Rockford, IL). Methods used were as described by us previously (Chen and Reith, 2008 and Li et al., 2010). Primary antibodies (mouse) were anti-MYC 9E10 (Santa Cruz Biotechnology, Dallas, TX; 1:500), anti-FLAG M2 antibody (Sigma-Aldrich, St. Louis, MO; 1:200), and anti-tubulin (Millipore, Temecula, CA; 1:5000). Secondary anti-mouse IgG antibody was from Thermoscientific (Rockford, IL). Immunoreactive protein bands were visualized with autoradiography film (Denville Scientific, South Plainfield, NJ). Films were scanned and band intensities were analyzed by densitometry using Image J software (National Institutes of Health, Bethesda, MD). To examine the amount of surface Myc- or Flag-tagged DAT compared to total DAT expression, the densitometric value for surface

DAT was divided by the densitometric value for total DAT normalized to tubulin. Flag-DAT WT was set as 100% for normalization.

In preparing the present work for publication, the guide for ethical behavior in publishing research was followed as described in the COPE Report 2003 (available from the Committee on Publication Ethics (COPE)).

Results and Discussion

Co-expression experiments for studying DAT oligomers

For detecting a change in the phenotype of DAT oligomers upon changing the protomer composition, we combined DAT constructs displaying different affinities for [^{3}H]CFT: W84L and D313N which have a lower K_d than WT; D345N and D436N which have a higher K_d than WT (Chen et al., 2001; 2004a; 2004b). Please see our previous report showing the formation of oligomers between these DAT constructs by co-immunoprecipitation and cross-linking approaches (Li et al., 2010). In the present experiments, as in our previous work, cells were transiently co-transfected with differentially tagged DAT constructs by the application of 1:1 ratios of cDNA amounts. Previously, we showed that Flag- and Myc-DAT were equally expressed in total lysates of preparations co-transfected in this manner (Li et al., 2010). Here we show that co-expression of WT DAT and W84L does not affect expression of each other at the cell surface (Figs. 1A and B). The same conclusion can be drawn for all paired constructs in this work by examining the B_{max} values of [^{3}H]CFT binding for separately and dually transfected cells (see below). As we have reported previously, the B_{max} value of [^{3}H]CFT binding to intact cells is a measure of binding primarily to surface DAT because CFT binds poorly in the intracellular milieu at high K^+ and low Na^+ and because intact cell [^{3}H]CFT binding can be completely inhibited by the impermeant substrate MPP^+ (Chen et al., 2004b). The conclusion that surface DAT expression is similar for the different constructs is obviously important in the present analysis because of the need to avoid having the oligomer phenotype dominated by one of the two constructs used for pairing. One could argue it is also important in view of reports that inhibitor potency to some extent is a function of DAT expression at the surface (Surratt et al., 2007; Chen and Reith, 2007). However, this phenomenon is observed only in functional transport experiments and not in radioligand binding experiments such as those conducted here (Surratt et al., 2007; Chen and Reith, 2007).

Validation of approach for detecting interacting DAT protomers: mixing experiments

The goal of the present study was to assess whether the binding properties in co-transfected cells (where oligomers containing the two different constructs can occur) differ from those in preparations obtained by mixing cells that had been separately transfected (where such oligomers cannot occur). Here we describe a method that replaces laborious “mixing” experiments with an *in silico* method predicting binding parameters from those observed for the singly expressed constructs. In the first set of experiments, a HEK-293 cell suspension stably expressing a single-type construct was mixed with a suspension expressing another single-type construct and assayed for [^{3}H]CFT binding alongside the single-construct

suspensions. For a given combination of DAT constructs, the total binding predicted to occur to non-interacting protomers at each concentration of CFT (2, 6, 14, 30, or 100 nM) was computed from the average binding parameters (K_d and B_{max}) of the singly expressed constructs as described in Materials and Methods. For graphical representation in a Scatchard plot, the bound over free values for these points were also calculated and can be seen for the example of mixing WT and W84L expressing cell suspensions (see solid red squares on "predicted non-interacting" curve in Fig. 1C). The same example includes the entire predicted non-interacting Scatchard plot (red line) calculated for numerous binding points with bound ligand values between 0 and 0.65 pmol/mg protein, as well as the lines (black) representing the binding for WT and W84L (along with their average data points, Fig. 1C; please note that the straight lines represent the average K_d and B_{max} obtained by nonlinear computer fitting of separate experiments whereas the data points are average values for bound/free and bound). The *in silico* generated data points for 2, 6, 14, 30, and 100 nM CFT (red squares) were subjected to RADLIG analysis to simulate an actual binding experiment on co-present DAT constructs forming hetero-oligomers consisting of non-interacting protomers, giving a predicted K_d of 4.72 nM and a Bmax of 0.60 pmol/mg (one-site binding; RADLIG analysis did not indicate a statistically better fit for 2 sites; see Table 1). When cell suspensions singly expressing WT and W84L were mixed and then assayed for binding, a one-site binding K_d of 5.33 nM and B_{max} of 0.54 pmol/mg protein was observed (Table 1), yielding a line (green, along with green averaged data points, Fig. 1C) in the Scatchard plot similar to the line (red) representing the *in silico* calculation for separate non-interacting constructs. In this combination of constructs with relatively high and low affinity of [^{3}H]CFT binding, the Scatchard curve predicted for the two binding components together displayed a slight hint of curvature (Fig. 1C, red line). The separation between high and low affinity was too small to generate two-site binding results with statistical significance in the RADLIG analysis. It remains to be seen whether increasing the number of data points beyond the current five would allow a two-site resolution for the pairs of constructs chosen here. It should be noted that the literature reporting two-site binding with curved Scatchard plots generally addresses nanomolar high-affinity binding in the presence of micromolar low-affinity binding, or binding components that are at least 10-fold or more different in their affinity (see Reith, 1986; Reith and Coffey, 1994). The present findings for all combinations tested were similar to the example shown in Fig. 1C, in that data points for combined or co-expressing cells essentially fell on a straight line describing homogeneous binding with one K_d value (see Figs. 1C and 2, red solid squares). It was also evident that the one-site binding predicted (or observed upon "mixing") for a given combination always had an affinity closer to that of the high-affinity population than to the numerical average of the co-present high- and low-affinity K_d.

To further validate the approach chosen to compare observed with predicted binding parameters, we mixed WT with D436N, and W84L with D345N, again pairing a higher with a lower affinity, respectively, with the expectation that mixing the different constructs yields a final binding pattern not different from that predicted *in silico* from the sum of the individually observed binding patterns. Indeed, as shown in Table 1, the observed values of K_d and B_{max} upon mixing were not statistically different from those predicted from combining the binding properties of the individual constructs *in silico*.

Detection of interacting DAT protomers: co-expression experiments

The above results establish the *in silico* prediction method as a valid approach for arriving at the binding parameters to be expected if hetero-oligomers consist of non-interacting protomers. The advantage of this method is that any combination of constructs can now be tested without having to simultaneously perform laborious mixing experiments with cell suspensions expressing the single-type constructs. Thus in the following, cells were co-transfected with various pairs of constructs with different binding affinities, and, in parallel, cells were transfected with single-type construct. In these experiments, transiently transfected cells were used. Predicted binding patterns for non-interacting protomers were calculated with the methods described above, and compared with binding observed upon co-expression. Fig. 2a shows the Scatchard plots for the pair WT with D436N, and Fig. 2b the pair WT with W84L. In comparing "predicted noninteracting" curves with "observed co-expressed" curves, one perceives a greater disparity between the prediction for non-interacting protomers and the observed result for the pair WT-D436N than for WT-W84L (compare Figs. 2a and b). All pairs tested are shown in Table 2, indicating statistically significant interactions between protomers of WT and D313N, WT and D345N, and WT and D436N. The statistically significant differences occurred in the K_d, not B_{max}, values with one exception (the latter showing a difference for WT with D345N) (Table 2). For each of the three pairs, the affinity changes were 1.7-, 2.2- and 4.1-fold, respectively. These results importantly indicate cooperativity within the hetero-oligomer.

Functional role of oligomers of biogenic amine transporters

The results obtained so far indicate that, under some, but not all, circumstances one protomer can influence the properties of another protomer of DAT. Available evidence suggests that DAT, as the related serotonin transporter (SERT), can exist as a tetramer (Kilic and Rudnick 2000; Milner *et al.* 1994; Hastrup *et al.* 2003). It is reasonable to think that interactions between protomers occur within each of the two dimers in the tetramer. The mutants that showed interactive effects in the present experiments were all conformationally biased: D313N has a greater proportion of outward-facing states than WT (Chen *et al.* 2004b; Liang *et al.* 2009), whereas D345N and D436N display a greater proportion of inward-facing states than WT (Chen *et al.* 2004a; Li *et al.* 2010). It is intriguing to note that the outward bias of D313N, causing its higher CFT binding affinity (Chen *et al.* 2004b; Schmitt *et al.* 2008), also resulted in a higher affinity under conditions allowing oligomers containing D313N with WT as compared with conditions where D313N and WT were present without interacting with each other. Conversely, the inward bias of D345N and D436N, causing their lower CFT binding affinity, was accompanied by a lower affinity when oligomers containing these constructs could be formed (Table 2). Such correspondence, however, was not ubiquitous as oligomers with WT and W84L, which has an outward bias, displayed intermediate WT-W84L affinity. We also do not have enough knowledge regarding the interfaces between DAT protomers to predict how conformational changes in one protomer affect the structure of the associated protomer. The size of the oligomer may also affect the protomer interactions. In this regard, a recent study shows the co-existence of different degrees of oligomerization at the cell surface for SERT (Anderluh et al., 2014a). The distribution of oligomeric states may be defined by some unknown

mechanism in the endoplasmic reticulum, and experiments tracking single SERT molecules in the ER have begun (Anderluh et al., 2014b).

This is the first report of an influence of protomer composition on the properties of a DAT inhibitor. If the observed effects are indeed related to conformational changes, one can consider the possibility that transport activity in one protomer with accompanying changes from outward to inward states (and back) influences the affinity of the other protomer for inhibitors. It is also possible that activity in one protomer shuts down transport by the associated protomer as suggested for the serotonin and norepinephrine transporters (Kilic and Rudnick 2000; Kocabas *et al.* 2003; Larsen *et al.* 2011), and the inhibitor changes observed in this work may just be indicators of structural changes in the associated protomer related to this shutdown.

Acknowledgments

This study was supported by a grant from the National Institutes of Health National Institute on Drug Abuse (R01 DA019676 to MEAR).

The abbreviations used are

DA	dopamine
DAT	dopamine transporter
CFT	(−)-2-β-carbomethoxy-3-β-(4-fluorophenyl)tropane
HEK	human embryonic kidney

References

Anderluh A, Klotzsch E, Reismann AW, Brameshuber M, Kudlacek O, Newman AH, Sitte HH, Schutz GJ. Single molecule analysis reveals coexistence of stable serotonin transporter monomers and oligomers in the live cell plasma membrane. J Biol Chem. 2014a; 289:4387–4394. [PubMed: 24394416]

Anderluh A, Klotzsch E, Ries J, Reismann AW, Weber S, Folser M, Koban F, Freissmuth M, Sitte HH, Schutz GJ. Tracking single serotonin transporter molecules at the endoplasmic reticulum and plasma membrane. Biophys J. 2014b; 106:L33–L35. [PubMed: 24806941]

Berger SP, Farrell K, Conant D, Kempner ES, Paul SM. Radiation inactivation studies of the dopamine reuptake transporter protein. Mol Pharmacol. 1994; 46:726–731. [PubMed: 7969052]

Billaud G, Costentin J, Bonnet JJ. Specific binding of [3H]GBR 12783 to the dopamine neuronal carrier included in polarized membranes. Eur J Pharmacol. 1993; 247:333–340. [PubMed: 8307105]

Chen N, Vaughan RA, Reith MEA. The role of conserved tryptophan and acidic residues in the human dopamine transporter as characterized by site-directed mutagenesis. J Neurochem. 2001; 77:1116–1127. [PubMed: 11359877]

Chen N, Reith MEA. Interaction between dopamine and its transporter: role of intracellular sodium ions and membrane potential. J Neurochem. 2004; 89:750–765. [PubMed: 15086531]

Chen N, Reith MEA. Substrates dissociate dopamine transporter oligomers. J Neurochem. 2008; 105:910–920. [PubMed: 18088380]

Chen N, Rickey J, Berfield JL, Reith MEA. Aspartate 345 of the dopamine transporter is critical for conformational changes in substrate translocation and cocaine binding. J Biol Chem. 2004a; 279:5508–5519. [PubMed: 14660644]

Chen N, Vaughan RA, Reith MEA. The role of conserved tryptophan and acidic residues in the human dopamine transporter as characterized by site-directed mutagenesis. J Neurochem. 2001; 77:1116–1127. [PubMed: 11359877]

Chen N, Zhen J, Reith MEA. Mutation of Trp84 and Asp313 of the dopamine transporter reveals similar mode of binding interaction for GBR 12909 and benztropine as opposed to cocaine. J Neurochem. 2004b; 89:853–864. [PubMed: 15140185]

Hastrup H, Karlin A, Javitch JA. Symmetrical dimer of the human dopamine transporter revealed by cross-linking Cys-306 at the extracellular end of the sixth transmembrane segment. Proc Natl Acad Sci U S A. 2001; 98:10055–10060. [PubMed: 11526230]

Hastrup H, Sen N, Javitch JA. The human dopamine transporter forms a tetramer in the plasma membrane: cross-linking of a cysteine in the fourth transmembrane segment is sensitive to cocaine analogs. J Biol Chem. 2003; 278:45045–45048. [PubMed: 14519759]

Just H, Sitte HH, Schmid JA, Freissmuth M, Kudlacek O. Identification of an additional interaction domain in transmembrane domains 11 and 12 that supports oligomer formation in the human serotonin transporter. J Biol Chem. 2004; 279:6650–6657. [PubMed: 14660642]

Kilic F, Rudnick G. Oligomerization of serotonin transporter and its functional consequences. Proc Natl Acad Sci U S A. 2000; 97:3106–3111. [PubMed: 10716733]

Kitayama S, Ikeda T, Mitsuhata C, Sato T, Morita K, Dohi T. Dominant negative isoform of rat norepinephrine transporter produced by alternative RNA splicing. J Biol Chem. 1999; 274:10731–10736. [PubMed: 10196144]

Kocabas AM, Rudnick G, Kilic F. Functional consequences of homo- but not hetero-oligomerization between transporters for the biogenic amine neurotransmitters. J Neurochem. 2003; 85:1513–1520. [PubMed: 12787070]

Kurian MA, Zhen J, Cheng SY, Li Y, Mordekar SR, Jardine P, Morgan NV, Meyer E, Tee L, Pasha S, Wassmer E, Heales SJ, Gissen P, Reith MEA, Maher ER. Homozygous loss-of-function mutations in the gene encoding the dopamine transporter are associated with infantile parkinsonism-dystonia. J Clin Invest. 2009; 119:1595–1603. [PubMed: 19478460]

Larsen MB, Sonders MS, Mortensen OV, Larson GA, Zahniser NR, Amara SG. Dopamine transport by the serotonin transporter: a mechanistically distinct mode of substrate translocation. J Neurosci. 2011; 31:6605–6615. [PubMed: 21525301]

Li Y, Cheng SY, Chen N, Reith MEA. Interrelation of dopamine transporter oligomerization and surface presence as studied with mutant transporter proteins and amphetamine. J Neurochem. 2010; 114:873–885. [PubMed: 20492355]

Liang YJ, Zhen J, Chen N, Reith MEA. Interaction of catechol and non-catechol substrates with externally or internally facing dopamine transporters. J Neurochem. 2009; 109:981–994. [PubMed: 19519772]

Milner HE, Beliveau R, Jarvis SM. The in situ size of the dopamine transporter is a tetramer as estimated by radiation inactivation. Biochim Biophys Acta. 1994; 1190:185–187. [PubMed: 8110814]

Reith MEA. Binding of [3H]imipramine to mouse cerebrocortical membranes and to glass fiber filters. J Neurochem. 1986; 46:760–766. [PubMed: 3950606]

Reith MEA, Coffey LL. [3H]WIN 35,428 binding to the dopamine uptake carrier. II Effect of membrane fractionation procedure and freezing. J Neurosci Methods. 1994; 51:31–38. [PubMed: 8189748]

Rosenthal HE. A graphic method for the determination and presentation of binding parameters in a complex system. Anal Biochem. 1967; 20:525–532. [PubMed: 6048188]

Schmitt KC, Reith MEA. The atypical stimulant and nootropic modafinil interacts with the dopamine transporter in a different manner than classical cocaine-like inhibitors. PLoS ONE. 2011; 6:e25790. [PubMed: 22043293]

Schmitt KC, Zhen J, Kharkar P, Mishra M, Chen N, Dutta AK, Reith MEA. Interaction of cocaine-, benztropine-, and GBR12909-like compounds with wild-type and mutant human dopamine transporters: molecular features that differentially determine antagonist-binding properties. J Neurochem. 2008; 107:928–940. [PubMed: 18786172]

Sitte HH, Farhan H, Javitch JA. Sodium-Dependent Neurotransmitter TRANSPORTERS: OLIGOMERIZATION as a Determinant of Transporter Function and Trafficking. Mol Intervent. 2004; 4:38–47.

Sitte HH, Freissmuth M. Oligomer formation by Na+-Cl--coupled neurotransmitter transporters. Eur J Pharmacol. 2003; 479:229–236. [PubMed: 14612153]

Sorkina T, Doolen S, Galperin E, Zahniser NR, Sorkin A. Oligomerization of dopamine transporters visualized in living cells by fluorescence resonance energy transfer microscopy. J Biol Chem. 2003; 278:28274–28283. [PubMed: 12746456]

Torres GE, Carneiro A, Seamans K, Fiorentini C, Sweeney A, Yao WD, Caron MG. Oligomerization and trafficking of the human dopamine transporter. Mutational analysis identifies critical domains important for the functional expression of the transporter. J Biol Chem. 2003; 278:2731–2739. [PubMed: 12429746]

Ukairo OT, Ramanujapuram S, Surratt CK. Fluctuation of the dopamine uptake inhibition potency of cocaine, but not amphetamine, at mammalian cells expressing the dopamine transporter. Brain Res. 2007; 1131:68–76. [PubMed: 17169338]

Zhen J, Chen N, Reith MEA. Differences in interactions with the dopamine transporter as revealed by diminishment of Na(+) gradient and membrane potential: Dopamine versus other substrates. Neuropharmacol. 2005; 49:769–779.

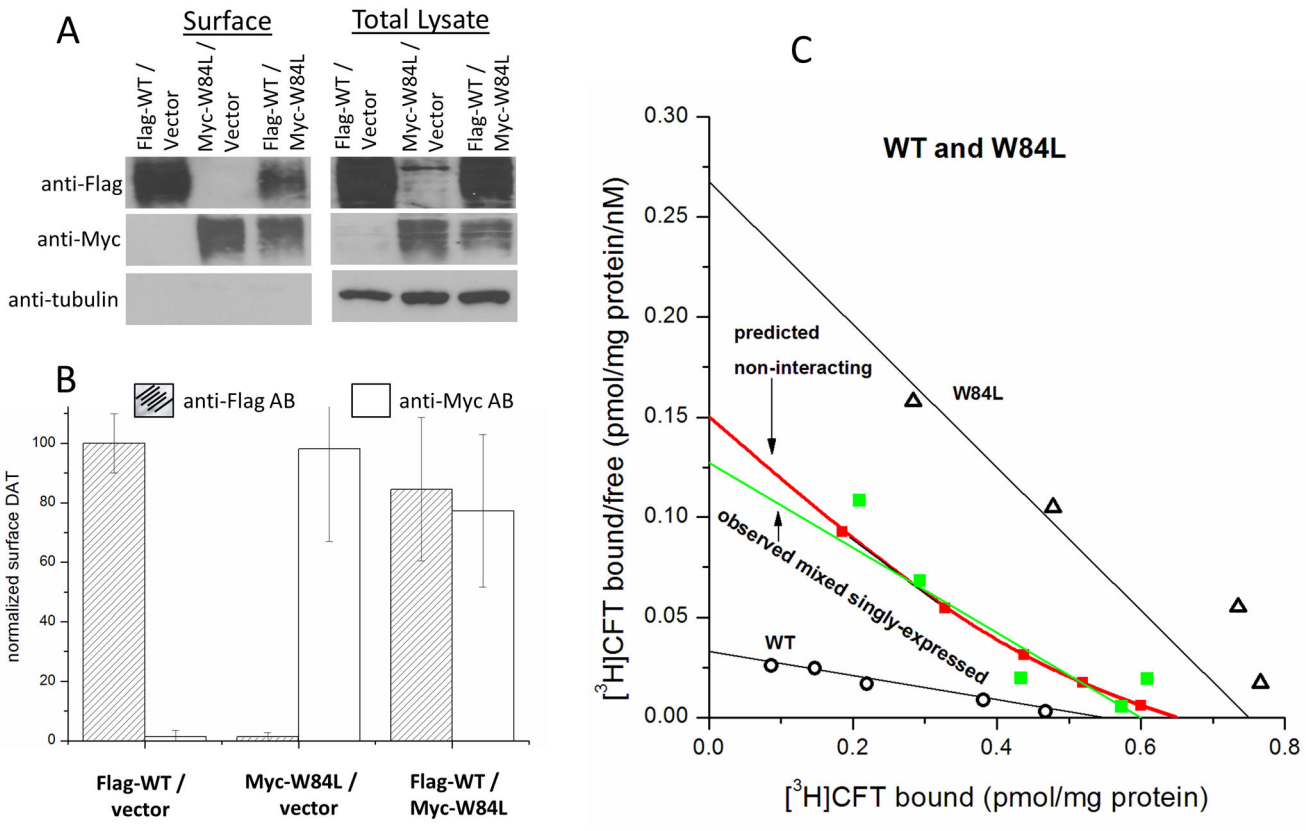

Fig. 1.

Method validation experiments for pairs of WT with W84L DAT. Panel A: Expression of WT DAT, W84L DAT, or both upon transient transfection. HEK 293 cells were transiently transfected with 5μg of plasmid DNA for Flag-WT or Myc-W84L DAT or vector (pcDNA3.1), or cotransfected with Flag-WT and Myc-W84L. 15 μg of total lysate was used to detect DAT and tubulin expression. WT, W84L, and tubulin were detected with anti-Flag antibody (AB), anti-Myc AB, and anti-tubulin AB, respectively. Blots are representative of experiments averaged in next panel. Panel B: Quantification of the data set that includes the gels shown in panel A. The densitometric value for surface Flag- or Myc-tagged DAT was divided by the densitometric value for total DAT expression normalized to tubulin. Flag-DAT WT was set as 100% for normalization. Results shown are average ± SEM for 3 experiments. Panel C: Saturation analysis of [^{3}H]CFT binding to WT and W84L DAT presented as Scatchard plots. Black lines depict the binding parameters for cells expressing the single-type constructs (see Table 1 for values), and the green line represents the binding parameters observed upon mixing cells singly expressing WT and W84L. The red line depicts the binding parameters computed from the average parameters of the singly expressed constructs for the case of non-interacting protomers. The solid red squares on this curve indicate the predicted binding at 2, 6, 14, 30, and 100 nM CFT, and, in mimicking a mixing experiment *in silico*, these values were used for the prediction of K_d and B_{max} given in Table 1. The straight black and green lines represent the average K_d and B_{max} obtained by nonlinear computer fitting of separate experiments whereas the black and green data points are average values for bound/free and bound.

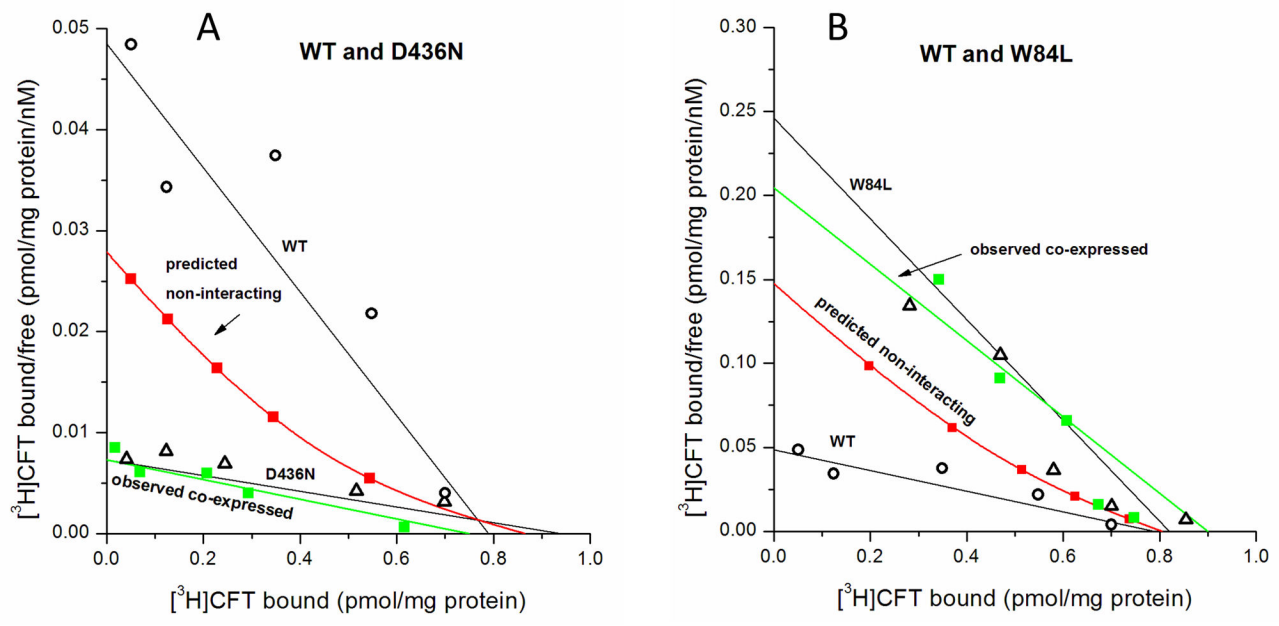

Fig. 2.

Saturation analysis of [^{3}H]CFT binding to WT and W84L DAT (panel A) and to WT and D436N DAT (panel B) presented as Scatchard plots. Black lines depict the binding parameters for cells expressing the single-type constructs (see Table 2 for values), and the green line represents the binding parameters observed in cells co-expressing two different constructs. The red line depicts the binding parameters computed from the average parameters of the singly expressed constructs for the case of non-interacting protomers. The solid red squares on this curve indicate the predicted binding at 2, 6, 14, 30, and 100 nM CFT, and, in mimicking a mixing experiment *in silico*, these values were used for the prediction of K_d and B_{max} given in Table 2. Otherwise details are as for Fig. 1C.

Table 1

Validation of *in silico* approach for detecting interacting protomers: Comparison of observed and predicted binding parameters upon mixing cells stably expressing separate DAT constructs

	Observed upon mixing cells expressing single constructs					**Predicted for non-interacting protomers**	
	WT	**W84L**	**WT + W84L**	**D436N**	**WT + D436N**	**WT + W84L**	**WT + D436N**
K_d, nM	16.8 ± 1.7 (6)	2.80 ± 0.42 (8)	5.33 ± 0.95 (3)	99.9 ± 4.1 (4)	25.9 ± 4.0 (4)	4.72 ± 0.35	24.1 ± 1.3
B_{max}, pmol/mg	0.55 ± 0.03 (6)	0.75 ± 0.16 (8)	0.54 ± 0.15 (3)	0.50± 0.08 (4)	0.38 ± 0.09 (4)	0.60 ± 0.02	0.44 ± 0.02
	W84L	D345N	W84L + D345N			W84L + D345N	
K_d, nM	2.80 ± 0.42 (8)	59.8 ± 7.2 (4)	2.01 ± 0.67 (3)			4.63 ± 0.68	
B_{max}, pmol/mg	0.75 ± 0.16 (8)	0.57 ± 0.13 (4)	0.77 ± 0.27 (3)			0.52 ± 0.03	

Cells stably expressing the indicated DAT constructs were mixed in equal volumes and worked up for [^{3}H]CFT binding measurements. Observed data are given as mean ± SE for the number (n) of independent experiments indicated in parentheses. Predicted values for non-interacting protomers were calculated from observed data for the non-mixed single constructs by performing nonlinear computer fitting on data points mimicking a binding experiment on mixed cells (see Materials and Methods). Predicted binding parameters obtained from this fitting by the “LIGAND” program are given as mean ± SE with the latter error estimate computed in nonlinear regression analysis based on minimizing the sum of the squares (RADLIG manual, Biosoft, Ferguson, MO, USA); these measures are based on the n experiments reported for the single constructs paired in the mixing experiments (on the left in the table). There are no statistical differences between observed and corresponding predicted values (one-sample Student’s t-test).

Table 2

Detection of interacting DAT protomers upon transiently co-transfecting cells with differential DAT constructs: Comparison of observed and predicted binding parameters

	Observed in singly- and co-transfected cells					**Predicted for non-interacting protomers**	
	WT	**W84L**	**WT + W84L**	**D313N**	**WT + D313N**	**WT + W84L**	**WT + D313N**
K_d, nM	16.3 ± 3.0 (4)	3.33 ± 0.45 (5)	4.40 ± 0.77 (3)	6.58 ± 0.46 (4)	6.42 ± 1.10 (5)*	5.87 ± 0.39	11.0 ± 0.03
B_{max}, pmol/mg	0.79 ± 0.21 (4)	0.82 ± 0.14 (5)	0.90 ± 0.25 (3)	0.41± 0.03 (4)	0.62 ± 0.11 (5)	0.76 ± 0.02	0.58 ± 0.01
	WT	D345N	WT + D345N	D436N	WT + D436N	WT + D345N	WT + D436N
K_d, nM	16.3 ± 3.0 (4)	48.8 ± 2.3 (4)	48.2 ± 10.3 (5)*	129 ±16 (3)	103 ± 5 (3)**	22.1 ±0.1	24.9 ± 1.8
B_{max}, pmol/mg	0.79 ± 0.21 (4)	0.62 ± 0.10 (4)	0.27 ± 0.04 (5)*	0.94 ± 0.04 (3)	0.75 ± 0.11 (3)	0.66 ± 0.01	0.66 ±0.03
	W84L	D345N	W84L + D345N			W84L + D345N	
K_d, nM	3.69 ± 0.44 (7)	46.9 ± 4.0 (6)	6.75 ± 3.22 (4)			5.36 ±0.50	
B_{max}, pmol/mg	0.94 ± 0.13 (7)	0.51 ± 0.12 (6)	1.40 ± 0.50 (4)			0.62 ± 0.02	

Cells were transiently transfected with the indicated single or dual constructs as described in Methods. For each 10-cm plate, 16 μg of cDNA was used, i.e. 8 μg each in the case of transfection with dual constructs. Observed data are given as mean ± SE for the number of independent experiments indicated in parentheses. Predicted values for non-interacting protomers were calculated from observed data for the single-construct expressing cells by performing nonlinear computer fitting on data points mimicking a binding experiment on mixed cells (see Materials and Methods). Predicted binding parameters are expressed as in Table 1.

* $p < 0.05$,

** $P < 0.005$ vs. corresponding predicted value (one-sample Student's t-test).